PHYSICAL REVIEW B **87**, 035117 (2013)

Noncollinear density functional theory having proper invariance and local torque properties

Ireneusz W. Bulik*
Department of Chemistry, Rice University, Houston, Texas 77005, USA

Giovanni Scalmani and Michael J. Frisch
Gaussian, Inc., 340 Quinnipiac Street, Building 40, Wallingford, Connecticut 06492, USA

Gustavo E. Scuseria
Department of Chemistry and Department of Physics and Astronomy, Rice University, Houston, Texas 77005, USA

(Received 31 October 2012; published 11 January 2013)

Noncollinear spins are among the most interesting features of magnetic materials, and their accurate description is a central goal of density functional theory applied to periodic solids. However, these calculations typically yield a magnetization vector that is everywhere parallel to the exchange-correlation magnetic field. No meaningful description of spin dynamics can emerge from a functional constrained to have vanishing local magnetic torque. In this contribution we present a generalization to periodic systems of the extension of exchange-correlation functionals to the noncollinear regime, proposed by Scalmani and Frisch [J. Chem. Theory Comput. **8**, 2193 (2012)]. This extension does afford a nonvanishing local magnetic torque and is free of numerical instabilities. As illustrative examples, we discuss frustrated triangular and kagome lattices evaluated with various density functionals, including screened hybrid functionals.

DOI: 10.1103/PhysRevB.87.035117 PACS number(s): 71.15.Mb

I. INTRODUCTION

The significance of density functional theory (DFT) in condensed-matter physics and quantum chemistry cannot be overstated. Its low computational cost, combined with increasingly accurate approximations to the exchange-correlation energy, constitute a powerful theoretical tool. The currently available functionals, although very successful in predicting the electronic structure of matter, are not yet general enough to be applicable for large classes of phenomena. One particular limitation of DFT is connected with the specific way the exchange-correlation (XC) functionals are constructed, namely, within the spin-polarized formalism.[1,2] In this approach, the dependence of the energy on the spin magnetization is introduced by an external magnetic field of vanishing magnitude, aligned along what, by convention, we call the z axis of spin quantization. Therefore, the density functionals depend solely on the total density n and the z component (i.e., the magnitude) of the magnetization vector, or, equivalently, the spin-up and spin-down densities, $n_\uparrow$ and $n_\downarrow$:

$$E[n,\vec{m}] \rightarrow E[n,m_z] \equiv E[n_\uparrow,n_\downarrow].$$

Even though collinear spin-polarized DFT (SDFT) suffices to describe many magnetic systems, this approximation cannot be applied in the case where the direction of the local magnetization is not constrained to a particular axis but can vary over the space. This type of behavior is known and has been observed in, for example, bulk γ-Fe, geometrically spin-frustrated lattices as jarosites, halogen salts of erbium, and surfaces.[3–10]

The nontrivial problem of going beyond collinear SDFT to account for spin noncollinearity has been of much recent concern. Even though the extension can be formally derived in terms of the total density and the full magnetization vector,[11] this approach has not yet directly benefited from the knowledge and experience accrued in the development of collinear SDFT functionals. The most common approach is to retain the form of the existing density functional approximations but to modify the basic ingredients of the theory. The spin densities are transformed to alternative quantities which carry the information about the magnetization. In other words, $E[n,\vec{m}]$ becomes $E[n_+,n_-]$. This approach was pioneered by Kübler *et al.*[12] for the local spin-density approximation (LSDA),[1] where the total spin density $\bar{n} = 1/2(n\sigma_0 + \vec{m}\cdot\vec{\sigma})$ at given point in space is brought to diagonal form by a unitary transformation,

$$\bar{n}(\vec{r}) = \frac{1}{2}\begin{pmatrix} n(\vec{r})+m_z(\vec{r}) & m_x(\vec{r})-im_y(\vec{r}) \\ m_x(\vec{r})+im_y(\vec{r}) & n(\vec{r})-m_z(\vec{r}) \end{pmatrix} \rightarrow \begin{pmatrix} n_+(\vec{r}) & 0 \\ 0 & n_-(\vec{r}) \end{pmatrix}, \quad (1)$$

which corresponds to finding a local reference frame where the magnetization is aligned along the z axis of spin quantization. The eigenvalues of the above matrix then take the place of spin densities and are $1/2(n \pm |\vec{m}|) = n_\pm$.

The extension of this formalism to more sophisticated density functional approximations has been reported by several authors. These approximations include the generalized gradient approximations (GGAs),[13] meta-GGAs, and hybrid functionals.[14,15] However, many of these extensions that directly rely on the local reference frame for density derivatives can suffer from numerical instabilities[14,16] or lead to an exchange-correlation magnetic field that is always parallel to the magnetization.[14] The exchange-correlation magnetic field is a functional derivative of the exchange-correlation energy with respect to the magnetization,

$$\vec{B}_{\rm xc}(\vec{r}) = \frac{\delta E[n,\vec{m}]}{\delta \vec{m}(\vec{r})}. \quad (2)$$

It is clear that this field cannot exert a global torque on the magnetization; hence it satisfies the zero torque theorem (ZTT).[17] However, $\vec{m}\times\vec{B}_{\rm xc}$ does not have to vanish identically at every

point in space. On the contrary, it has been shown that this local contribution plays a crucial role in describing spin dynamics. It has been pointed out that within the adiabatic approximation to time-dependent DFT, the density functionals that do not afford nonzero exchange-correlation torque cannot properly describe the time evolution of the magnetization.[18] Therefore, an extension of collinear SDFT to noncollinear DFT that satisfies the ZTT locally (by constraining $\vec{B}_{\rm xc}$ to be collinear to the magnetization) is not useful for such applications.

Recently, an extension of collinear SDFT was proposed by two of the present authors.[16] This approach not only is readily applicable to any existing functional including GGAs and meta-GGAs but also is free of the aforementioned collinearity constraint. Moreover, it does not suffer from the numerical instabilities that proved to be problematic in our previous formulation of noncollinear DFT.[14]

The purpose of this work is to provide a generalization of our formalism for periodic systems. It is well established that many properties of solids, such as band gaps and lattice parameters, are much more accurate when described in terms of screened hybrid functionals.[19–24] We thus describe here an extension of general spin-polarized exchange-correlation functionals that depend on nonlocal Hartree-Fock-type (exact) exchange to the noncollinear regime. As in previous work, we adopt a generalized Kohn-Sham (KS) approach[25–28] which is computationally more feasible than the optimized effective potential scheme reported in the literature[18] and does not suffer from discretization problems when used in connection with Gaussian orbitals.[29] Additionally, exact exchange is not constrained by any variable transformation, and hence its contribution, the exchange-correlation magnetic field, does not suffer problems connected to generalization of the DFT part. Therefore our formalism seems to be well suited for hybrid functionals. Furthermore, we provide a simple implementation scheme that allows us to extend Gaussian orbital-based collinear SDFT codes to the noncollinear regime. Noncollinear DFT requires a two-component treatment; thus our formalism can be combined with relativistic schemes going beyond scalar effects. In particular, vector spin-orbit effects can be easily included. Finally, we apply our approach to spin-frustrated lattices. We explicitly show that our formalism does not lead to locally vanishing exchange-correlation magnetic torque. Therefore we provide examples of Gaussian orbital-based noncollinear DFT self-consistent calculations of extended systems.

II. THEORY AND IMPLEMENTATION

A. Basic quantities

In order to allow for noncollinearity in Kohn-Sham DFT (KS-DFT), we start by expressing the nth crystalline orbital as a two-component spinor (x denotes spin and space coordinate),

$$\psi_n^{\vec{k}}(x) = \begin{pmatrix} \psi_n^{\alpha,\vec{k}}(\vec{r}) \\ \psi_n^{\beta,\vec{k}}(\vec{r}) \end{pmatrix},$$

where $\psi_n^{\sigma,\vec{k}}(\vec{r})$ are expanded in terms of Bloch functions,

$$\psi_n^{\sigma,\vec{k}}(\vec{r}) = \sum_\nu c_{\mu n}^{\sigma\vec{k}} \tilde{\phi}_\mu^{\vec{k}}(\vec{r}),$$

and

$$\tilde{\phi}_\mu^{\vec{k}}(\vec{r}) = \frac{1}{\sqrt{N}} \sum_{\vec{L}} e^{i\vec{k}\cdot\vec{L}} \phi_\mu^{\vec{L}}(\vec{r}),$$

where $\vec{L}$ is a vector pointing to the Lth (out of N) cell and $\phi_\mu^{\vec{L}}(\vec{r}) = \phi_\mu(\vec{r} - \vec{L})$ is the μth atomic orbital in this cell (we assume it to be a real function in what follows). The single-particle density matrix takes the following block structure (the sum over the band index should be understood as a sum over occupied bands):

$$\gamma(x,x') = \sum_{\vec{k}} \sum_n \psi_n^{\vec{k}}(x) \psi_n^{\vec{k}\dagger}(x') = \begin{pmatrix} \gamma^{\alpha\alpha}(\vec{r},\vec{r}') & \gamma^{\alpha\beta}(\vec{r},\vec{r}') \\ \gamma^{\beta\alpha}(\vec{r},\vec{r}') & \gamma^{\beta\beta}(\vec{r},\vec{r}') \end{pmatrix}.$$

Henceforth, we will drop the dependence on the electronic coordinate for brevity of notation, unless it could lead to confusion. As usual, $n = \mathrm{tr}_\sigma[\gamma]$, where the trace is to be understood in the spin space. Similarly ($\vec{\sigma}$ denotes the vector of Pauli matrices),

$$\vec{m} = \mathrm{tr}_\sigma[\vec{\sigma}\cdot\gamma] = \begin{pmatrix} \gamma^{\alpha\beta} + \gamma^{\beta\alpha} \\ i[\gamma^{\alpha\beta} - \gamma^{\beta\alpha}] \\ \gamma^{\alpha\alpha} - \gamma^{\beta\beta} \end{pmatrix} = \begin{pmatrix} m_x \\ m_y \\ m_z \end{pmatrix}. \tag{3}$$

Each block of the density matrix has the following representation in terms of Bloch functions ($\bar{z}$ denotes the complex conjugate of z):

$$\begin{aligned} \gamma^{\sigma\sigma'} &= \frac{1}{N} \sum_{\vec{L}\vec{L}'} \sum_{\mu\nu} \phi_\mu^{\vec{L}} \phi_\nu^{\vec{L}'} \sum_{\vec{k}} e^{i\vec{k}\cdot(\vec{L}-\vec{L}')} \sum_n c_{\mu n}^{\sigma\vec{k}} \bar{c}_{\nu n}^{\sigma'\vec{k}} \\ &= \sum_{\vec{L}\vec{L}'} \sum_{\mu\nu} \left[P_{\mu\nu}^{\sigma\sigma'}\right]^{\vec{L}\vec{L}'} \phi_\mu^{\vec{L}} \phi_\nu^{\vec{L}'}, \end{aligned} \tag{4}$$

which defines $[P_{\mu\nu}^{\sigma\sigma'}]^{\vec{L}\vec{L}'}$,

$$\left[P_{\mu\nu}^{\sigma\sigma'}\right]^{\vec{L}\vec{L}'} = \frac{1}{N} \sum_{\vec{k}} \sum_n c_{\mu n}^{\sigma\vec{k}} \bar{c}_{\nu n}^{\sigma'\vec{k}} e^{i\vec{k}\cdot(\vec{L}-\vec{L}')}.$$

As usual, the summation over the Brillouin zone can be approximated with an integral. The density matrix naturally takes the following spin structure:

$$\begin{pmatrix} \mathbf{P}^{\alpha\alpha} & \mathbf{P}^{\alpha\beta} \\ \mathbf{P}^{\beta\alpha} & \mathbf{P}^{\beta\beta} \end{pmatrix}^{\vec{L}\vec{L}'}. \tag{5}$$

The periodic symmetry and the Hermiticity of the infinite real-space density matrix implies that $(\mathbf{P}^{\vec{L}\vec{L}'})^\dagger = \mathbf{P}^{\vec{L}'\vec{L}}$. Hence,

$$\begin{pmatrix} (\mathbf{P}^{\alpha\alpha})^\dagger & (\mathbf{P}^{\beta\alpha})^\dagger \\ (\mathbf{P}^{\alpha\beta})^\dagger & (\mathbf{P}^{\beta\beta})^\dagger \end{pmatrix}^{\vec{L}\vec{L}'} = \begin{pmatrix} \mathbf{P}^{\alpha\alpha} & \mathbf{P}^{\alpha\beta} \\ \mathbf{P}^{\beta\alpha} & \mathbf{P}^{\beta\beta} \end{pmatrix}^{\vec{L}'\vec{L}}. \tag{6}$$

It is clear that the information encoded in the full $\mathbf{P}^{\vec{L}\vec{L}'}$ is redundant. Therefore, we perform the standard decomposition of an arbitrary matrix into its Hermitian and anti-Hermitian components, which later on can be further separated into real symmetric (RS), imaginary symmetric (IS), real antisymmetric (RA), and imaginary antisymmetric (IA) contributions. We propose here the following way of carrying out this

decomposition for periodic systems:

$$\left[\mathbf{P}_{RS}^{\sigma\sigma'}\right]^{\vec{L}\vec{L}'} = \tfrac{1}{2}[\mathrm{Re}(\mathbf{P}^{\sigma\sigma'} + \mathbf{P}^{\sigma'\sigma})]^{\vec{L}\vec{L}'} \quad (7)$$

$$\left[\mathbf{P}_{IA}^{\sigma\sigma'}\right]^{\vec{L}\vec{L}'} = \tfrac{1}{2}[\mathrm{Im}(\mathbf{P}^{\sigma\sigma'} + \mathbf{P}^{\sigma'\sigma})]^{\vec{L}\vec{L}'}. \quad (8)$$

Analogously, the RA and IS components are obtained by taking the difference in the equations above. We note that the symmetry or antisymmetry property of the above matrices should be understood in the sense that

$$P_{\nu\mu}^{\vec{L}\vec{L}'} = \pm P_{\mu\nu}^{\vec{L}'\vec{L}},$$

which can be readily verified using Eq. (6). Clearly, the same spin RA and IS blocks of density matrices vanish identically. Note that this decomposition allows one to limit the amount of data stored not only for the density matrix but also for each Hermitian matrix that obeys a relation analogous to Eq. (6). For instance, one only needs to construct the decomposition for, say, $\mathbf{P}^{\alpha\beta}$ for given vectors $\vec{L}$ and $\vec{L}'$. The corresponding block $\mathbf{P}^{\beta\alpha}$ can be always obtained for the cell $\vec{L}'$ and $\vec{L}$. Therefore, a set of only eight real matrices of dimension N suffices to reconstruct the full real-space complex density matrix of dimension $2N$.

B. Effective single-particle equations

Using the standard decomposition of the total energy in the KS scheme, the total energy per unit cell E can be written as

$$E = E_T + E_N + E_J + E_{\mathrm{xc}} + E_{\mathrm{SD}}, \quad (9)$$

where E_T is the kinetic energy, E_N is the electron-nuclei attraction and nuclei-nuclei repulsion energy, E_J is the classical Coulomb interaction of the electron density, and the exchange-correlation energy E_{xc} includes the quantum corrections. The last term describes the energy arising from additional spin-dependent interactions, for example, spin-orbit coupling. Variation of the energy expression with respect to crystalline orbitals leads to the following KS equations:

$$(\hat{t} + \hat{v}_N + \hat{j} + \hat{v}_{\mathrm{xc}} + \hat{h}_{\mathrm{SD}})\psi_n^{\vec{k}}(x) = \epsilon_k \psi_n^{\vec{k}}(x), \quad (10)$$

where $t = -\frac{1}{2}\nabla^2$.

The kinetic energy, together with the Coulombic part of the potential, $\hat{v}_N + \hat{j}$, is diagonal in spin space. Namely,

$$\hat{t} + \hat{v_N} + \hat{j} = \sigma_0\left(-\frac{1}{2}\nabla^2 - \sum_A \frac{Z_a}{|\vec{r} - \vec{R}_A|} + \int d\vec{r}\,' \frac{n(\vec{r}\,')}{|\vec{r} - \vec{r}\,'|}\right), \quad (11)$$

where A labels the atoms in the crystal and σ_0 is the 2×2 identity matrix. Whereas the kinetic energy integrals require no modification of the one-component code, the Coulombic part can be easily computed by providing the one-component routines with few $P^{\sigma\sigma}$ matrices. Restricting ourselves to a real Gaussian basis set, only the real symmetric part of these matrices must be used, which is clear from the symmetry of the two electron integrals. As usual, care must be taken when evaluating formally divergent terms in the Coulomb sums. In the present work we have used the Gaussian fast multipole method as presented by Kudin *et al.*[30–32]

Now, let us turn our attention to the exchange-correlation part. As mentioned in the Introduction, we wish to consider general XC approximations that contain a portion of exact (nonlocal) HF-type exchange. Therefore, we write

$$\hat{v}_{\mathrm{xc}} = a\hat{K} + (1 - a)\hat{v}_x^{\mathrm{DFT}} + \hat{v}_c^{\mathrm{DFT}},$$

where $\hat{K}$ is the Fock exchange operator and a is a mixing parameter. The underlying interaction does not have to correspond, however, to the bare Coulomb potential but can take, for instance, a screened (short-range) or a middle-range interaction.[33] Including all of the above in an operator $\hat{V}_{\mathrm{eff}}$, we write

$$\begin{aligned}\hat{K}\psi_n^{\vec{k}}(x) &= -\sum_{\vec{k}'}\sum_m \int d\vec{x}\,' \psi_m^{\vec{k}'}(x)\hat{V}_{\mathrm{eff}}\psi_m^{\vec{k}'\dagger}(x')\psi_n^{\vec{k}}(x') \\ &= -\int dx'\hat{V}_{\mathrm{eff}}\gamma(x,x')\psi_n^{\vec{k}}(x'). \end{aligned} \quad (12)$$

Expanding the two-component spinors in terms of the localized atomic orbitals, one easily finds that the matrix representation of the exchange operator takes a spin-blocked form analogous to the density matrix,

$$\mathbf{K}^{\vec{L}\vec{L}'} = \begin{pmatrix} \mathbf{K}^{\alpha\alpha} & \mathbf{K}^{\alpha\beta} \\ \mathbf{K}^{\beta\alpha} & \mathbf{K}^{\beta\beta} \end{pmatrix}^{\vec{L}\vec{L}'},$$

where

$$\left[K_{\mu\nu}^{\sigma\sigma'}\right]^{\vec{L}\vec{L}'} = \sum_{\lambda\kappa}\sum_{\vec{H}\vec{H}'}\left[P_{\lambda\kappa}^{\sigma\sigma'}\right]^{\vec{H}\vec{H}'}\langle\mu^{\vec{L}}\kappa^{\vec{H}'}|\lambda^{\vec{H}}\nu^{\vec{L}'}\rangle.$$

In order to perform the exchange integral contraction with minimal modification of our existing single-component periodic code, we use the decomposition of the density matrix established in the previous section. Each portion is a real matrix whose size is the same as in the single-component case. It is thus sufficient to contract the two electron integrals with each block of $\mathbf{P}$. Now, reversing the transformation of Eq. (7) allows us to reconstruct the full $\mathbf{K}$ matrix.

Finally, let us discuss the pure density functional part of the exchange-correlation energy. As mentioned in the Introduction, the extension of collinear SDFT to the noncollinear regime relies on the transformation of variables. Namely, a set of variables (denoted with subscript + and −) is obtained from the total density and magnetization vector and their gradients,

$$\{n,\vec{m}\} \rightarrow \{n_\pm,\gamma_\pm,\gamma_{\mathrm{mix}},\tau_\pm,\nabla^2 n_\pm\},$$

where $\gamma_\pm$ mimics the modulus square of the gradient of spin-up and -down densities, γ_{mix} is the cross term, $\tau_\pm$ substitutes the kinetic-energy density, and $\nabla^2 n_\pm$ substitutes the Laplacian. It should be understood that such a variable transformation is not unique. Nonetheless, we believe that the particular transformation introduced in Ref. 16 and employed here satisfies many important requirements: (i) it does not constrain the relative orientation of magnetization and exchange-correlation field, thereby allowing for a nonvanishing local magnetic torque while satisfying the global zero torque theorem,[17] (ii) both the XC energy and the intermediate variables are invariant with respect to spin rotations, (iii) a vanishingly small magnitude of the magnetization vector does not lead to numerical instabilities, and (iv) the proper collinear limit is recovered as all the spins align with respect to any arbitrary spin-quantization axis.

For completeness, we present below these transformations explicitly:

$$n_\pm = \frac{1}{2}[n \pm \sqrt{\vec{m}\circ\vec{m}}], \tag{13}$$

$$\gamma_\pm = \frac{1}{4}[\nabla n\cdot\nabla n + \nabla\vec{m}\circ\cdot\nabla\vec{m}] \pm \frac{f_\nabla}{2}\sqrt{(\nabla n\cdot\nabla\vec{m})\circ(\nabla n\cdot\nabla\vec{m})}, \tag{14}$$

$$\gamma_{\rm mix} = \frac{1}{4}[\nabla n\cdot\nabla n - \nabla\vec{m}\circ\cdot\nabla\vec{m}], \tag{15}$$

with $\circ$ $(\cdot)$ denoting a scalar product in spin (real) space and $f_\nabla = \mathrm{sgn}(\nabla n\cdot\nabla\vec{m}\circ\vec{m})$, with sgn being the signum function. The meta-GGA components are generalized as

$$\tau_\pm = \tfrac{1}{2}[\tau \pm f_\tau\sqrt{\vec{u}\circ\vec{u}}], \tag{16}$$

$$\nabla^2 n_\pm = \tfrac{1}{2}[\nabla^2 n \pm f_{\nabla^2}\sqrt{\nabla^2\vec{m}\circ\nabla^2\vec{m}}], \tag{17}$$

with $f_\tau = \mathrm{sgn}(\vec{u}\circ\vec{m})$ and $f_{\nabla^2} = \mathrm{sgn}(\nabla^2\vec{m}\circ\vec{m})$. The vector $\vec{u}$ is obtained by replacing γ by $1/2\nabla_{\vec{r}}\cdot\nabla_{\vec{r}'}\gamma(\vec{r},\vec{r}')|_{\vec{r}=\vec{r}'}$ in Eq. (3).

The extension of the one-component code is therefore straightforward. Translating Eq. (3) into the localized Gaussian basis, we construct

$$\begin{aligned}
n(\vec{r}) &= \sum_{\mu\nu}\sum_{\vec{L}\vec{L}'}\left(\mathbf{P}^{\alpha\alpha}_{RS}+\mathbf{P}^{\beta\beta}_{RS}\right)^{\vec{L}\vec{L}'}_{\mu\nu}\mu^{\vec{L}}(\vec{r})\nu^{\vec{L}'}(\vec{r}),\\
m_x(\vec{r}) &= 2\sum_{\mu\nu}\sum_{\vec{L}\vec{L}'}\left(\mathbf{P}^{\alpha\beta}_{RS}\right)^{\vec{L}\vec{L}'}_{\mu\nu}\mu^{\vec{L}}(\vec{r})\nu^{\vec{L}'}(\vec{r}),\\
m_y(\vec{r}) &= 2\sum_{\mu\nu}\sum_{\vec{L}\vec{L}'}\left(\mathbf{P}^{\alpha\beta}_{IS}\right)^{\vec{L}\vec{L}'}_{\mu\nu}\mu^{\vec{L}}(\vec{r})\nu^{\vec{L}'}(\vec{r}),\\
m_z(\vec{r}) &= \sum_{\mu\nu}\sum_{\vec{L}\vec{L}'}\left(\mathbf{P}^{\alpha\alpha}_{RS}-\mathbf{P}^{\beta\beta}_{RS}\right)^{\vec{L}\vec{L}'}_{\mu\nu}\mu^{\vec{L}}(\vec{r})\nu^{\vec{L}'}(\vec{r}).
\end{aligned} \tag{18}$$

Again, we have used the fact that we work with real atomic orbitals as the underlying basis. Furthermore, by tracing the above combination of density matrices with the gradients of basis functions, we can construct the gradient of the magnetization and higher derivatives in the usual way. The DFT contribution to the Fock matrix can now be explicitly formed by taking the derivatives of the exchange-correlation energy with respect to the density matrix,[25] with functional derivatives with respect to $\pm$ variables changed into derivatives with respect to n and $\vec{m}$ via the chain rule. Namely, the functional derivative with respect to, say, m_y is used just as in the one-component code to obtain the contributions to the imaginary symmetric block of the Fock matrix. This step takes place in the numerical quadrature and requires only minor modifications to the existing subroutines.

C. Analysis and visualization of the magnetization and the exchange-correlation magnetic field

The visualization of the magnetization vector field $\vec{m}(\vec{r})$ does not raise any particular issue since it is sufficient to use Eqs. (18) to map $\vec{m}(\vec{r})$ over any selected region of space.

The situation is different for $\vec{B}_{\rm xc}(\vec{r})$. In our implementation of the KS equations, we do not construct explicit functional derivatives of the energy with respect to the electron density. Instead, as mentioned in the Introduction, we take variations with respect to the one-particle density matrix. Therefore, in order to evaluate (and visualize) $\vec{B}_{\rm xc}(\vec{r})$ we actually performed the integration by parts[25] required to express the XC magnetic field as a local function involving only derivatives with respect to the magnetization density (18), leading to

$$\vec{B}_{\rm xc} = \frac{\delta E_{\rm xc}}{\delta\vec{m}} = \frac{\partial f}{\partial n_+}\frac{\partial n_+}{\partial\vec{m}} + \frac{\partial f}{\partial n_-}\frac{\partial n_-}{\partial\vec{m}} - \nabla\cdot\left(\frac{\partial f}{\partial\gamma_+}\frac{\partial\gamma_+}{\partial\nabla\vec{m}} + \frac{\partial f}{\partial\gamma_-}\frac{\partial\gamma_-}{\partial\nabla\vec{m}} + \frac{\partial f}{\partial\gamma_{\rm mix}}\frac{\partial\gamma_{\rm mix}}{\partial\nabla\vec{m}}\right), \tag{19}$$

where f is the density functional. The above expression is significantly more complex than what it is required to variationally minimize the energy with respect to the one-particle density matrix (5). In fact, it involves second derivatives of the functional and the full second derivatives of the magnetization densities (18). Moreover, in the case of a meta-GGA functional, the same integration by parts does not allow us to express the direct dependence of the energy on the kinetic-energy density (16) as a derivative with respect to $\vec{m}$. Therefore, Eq. (19) cannot be extended to meta-GGA. It also cannot be extended to hybrid functionals because the exact exchange is nonlocal in nature.

In addition to the ability of visualizing $\vec{m}(\vec{r})$ and $\vec{B}_{\rm xc}(\vec{r})$, another important interpretation tool for noncollinear DFT solutions is the partitioning of the total magnetization into atomic contributions. In the present work, we employ an extension of the Hirshfeld population analysis[34] to periodic systems. This approach, originally derived for calculating atomic charges, relies on the idea of describing the difference between nonbonded atoms and molecules. This analysis can be extended to other continuous variables as it partitions space into single atomic regions. In other words, in this scheme one defines a "procrystal" density that is composed of spherically averaged ground-state densities of the atoms of the crystal $\tilde{n}$,

$$n^{\rm pro}(\vec{r}) = \sum_{\vec{L}}\sum_{A}\tilde{n}_A(\vec{r}-\vec{L}),$$

where we split the summation over the unit cell replicas and atoms in the unit cell. We also define the sharing function $\tilde{u}_A$,

$$\tilde{u}^{\vec{L}}_A(\vec{r}) = \tilde{u}_A(\vec{r}-\vec{L}) = \frac{\tilde{n}_A(\vec{r}-\vec{L})}{n^{\rm pro}(\vec{r})}.$$

An integrated value Q of a given continuous quantity $q(\vec{r})$ can be therefore expressed as (u.c. denotes unit cell),

$$Q = \int_{u.c.} d\vec{r}\, q(\vec{r}) = \sum_A\sum_{\vec{L}}\int_{u.c.} d\vec{r}\, q(\vec{r})\tilde{u}^{\vec{L}}_A(\vec{r}).$$

Using the periodic symmetries of the quantity of interest and the sharing function, we change the integral over the unit cell to an integral over the whole space. Then,

$$Q = \sum_A\left[\int d\vec{r}\, q(\vec{r})\tilde{u}^{\vec{0}}_A(\vec{r})\right] = \sum_A Q_A,$$

where the sharing function is now centered in unit cell 0. This partitions the quantity Q into atomic components Q_A. In the actual calculation we also introduce the standard DFT

integration weights.[35] We applied the Becke weights modified by Stratmann *et al.*[36]

III. RESULTS AND DISCUSSION

A. Computational details

As a prototypical application of our methodology, we have studied two-dimensional spin-frustrated lattice models with chromium atoms at the nodes. The distance between individual atoms corresponds to the interatomic separation of the Ag(111) surface.[37] We have adopted this specific geometry following Ref. 18. For each lattice, we have carried out calculations employing a representative functional from each class of commonly used DFT approximations. For the local ones, we have used the LSDA with Dirac exchange and the Vosko, Wilk, and Nusair parametrization of correlation (SVWN5).[38] As a model GGA functional we have chosen the Perdew-Burke-Ernzerhof (PBE)[39] functional. For the meta-GGA we have chosen the Tao-Perdew-Staroverov-Scuseria (TPSS)[40] functional. From the hybrid functionals, we have employed two range-separated models, the Heyd-Scuseria-Ernzerhof (HSE)[19,20] and the Henderson-Izmaylov-Scuseria-Savin (HISS).[33] The former separates the exchange operator into short and long ranges, whereas the latter additionally introduces a middle range. We should stress at this point that our approach is readily applicable to any functional belonging to any of the above classes.

Even though our implementation supports spin-orbit coupling terms via relativistic core potentials, we have not included them in the present calculations. Instead, we have restricted ourselves to scalar-relativistic effective core potentials, substituting the Ne core of Dolg *et al.*[41] We have adapted the corresponding basis set to periodic calculations by removing basis functions with exponents below 0.095 bohr^{-2}. We have also neglected the g functions. All calculations were carried out using the GAUSSIAN suite of programs.[42] The default (tight) GAUSSIAN convergence criteria, which correspond to a convergence of at least 10^{-7} on the root-mean-square of the density matrix, has been used. The DFT numerical quadrature has been set to a pruned grid of 225 radial points and 974 angular points. The reciprocal space was sampled with 2116 points.

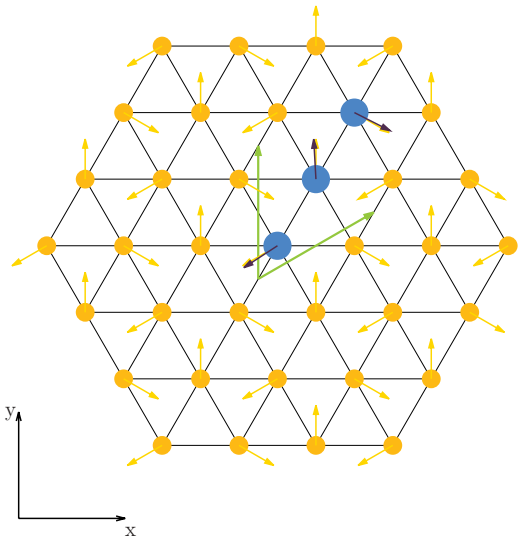

FIG. 1. (Color online) The structure of the triangular Cr lattice. The blue points represent the magnetic unit cell employed in the calculations. The dark blue arrows present the converged magnetization obtained with the HSE functional, partitioned according to the Hirshfeld scheme. Additionally, the translation vectors are presented (green arrows).

TABLE I. The calculated net magnetic moments of chromium atoms (in μ_B) for the lattices considered in this work.

	Functional				
	LSDA	PBE	TPSS	HSE	HISS
Triangular	2.11	2.15	2.18	2.26	2.15
Kagome $\vec{q} = 0$	2.25	2.29	2.32	2.37	2.28
Kagome $\sqrt{3} \times \sqrt{3}$	2.27	2.31	2.33	2.39	2.30

B. Triangular lattice

The first lattice that we have studied is a triangular one. It is known[18] that this system exhibits a noncollinear antiferromagnetic Néel state, where the magnetization around each of the lattice points in the magnetic unit cell is oriented at an angle of $2\pi/3$ with respect to each point. Not surprisingly, each of the tested functionals properly identified this state. We have observed good agreement between the ideal and computed angles between the atomic magnetization vectors. The geometry of the lattice is shown in Fig. 1.

Despite this qualitative agreement, the total value of the magnetization divided into atomic contributions reveals quantitative differences. The results are presented in Table I. We have observed that the total magnetic moment increases as one climbs Jacob's ladder of functionals,[43] with the exception of the HISS functional, which predicts the norm of the magnetization to be very similar to the PBE value. We note that the magnetic moment of the chromium atom obtained with

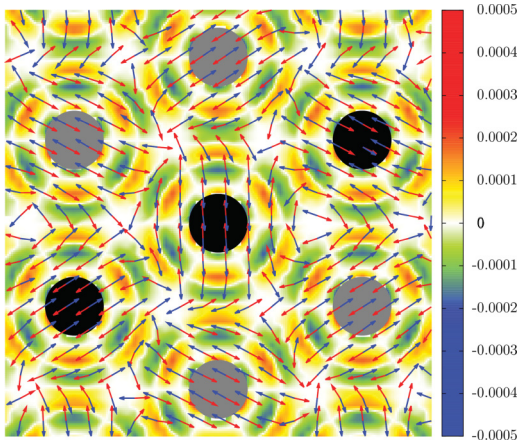

FIG. 2. (Color online) The directions of the magnetization (red arrows) and the exchange-correlation magnetic field (blue arrows) obtained with the PBE functional. The color map depicts the magnitude (in atomic units) of $\vec{m} \times \vec{B}_{\text{xc}}$ in the direction perpendicular to the Cr surface. The black points indicate the actual magnetic unit cell used in the calculations.

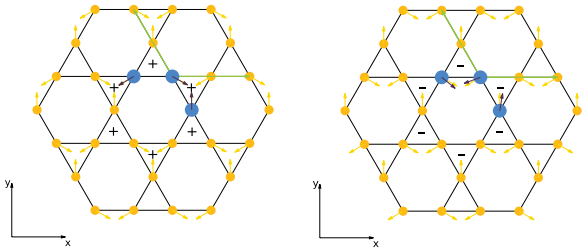

FIG. 3. (Color online) The structure of the kagome $\vec{q} = 0$ lattices of the (left) positive and (right) negative chiralities. The blue points represent the actual magnetic unit cell used in the calculations, with arrows representing the converged magnetization obtained with the HISS functional partitioned according to the Hirshfeld scheme. For the clarity of the picture, the magnetization for the negative chirality has been rotated to stress the difference to the left panel. Additionally, the translation vectors are presented (green arrows).

LSDA, $2.11\mu_B$, is in fairly good agreement with the value of $2.0\mu_B$ reported by Sharma *et al.*[18]

Now let us turn our attention to the key point of the present work, namely, abandoning the collinearity constraint between the local magnetization vector and the exchange-correlation magnetic field. Even though our formalism does not impose such a constraint on any of the functionals (except LSDA, where it naturally arises), we shall discuss this point only using pure GGA examples for the reason mentioned in Sec. II C. However, let us stress that exact exchange is fully nonlocal and unconstrained; therefore the problem of locally vanishing magnetic torque, $\vec{m} \times \vec{B}_{\rm xc}$, does not apply for the Hartree-Fock part of hybrid functionals. Additionally, calculations carried out within the optimized effective potential, where the local representation of the exchange-correlation magnetic field is accessible for exact exchange, have shown a nonvanishing local torque between $\vec{m}$ and $\vec{B}_{\rm xc}$.[18]

In Fig. 2 we present the local distribution of the aforementioned quantities obtained with the PBE functional. In the present work, we do not reverse the orientation of $\vec{B}_{\rm xc}$ with respect to $\vec{m}$, as we have done in Ref. 16. In analogy to previous studies,[14,18] we find that the magnetization tends to be highly collinear in the core region, with rather strongly accented boundaries where it changes orientation. These boundaries coincide with the domains where the calculated exchange-correlation magnetic field deviates the most from the collinear alignment with respect to $\vec{m}$. It is clear that the exchange-correlation magnetic torque is non-negligible and exhibits rich structure. This, obviously, cannot be captured by previous generalizations of GGA functionals to noncollinear SDFT, in which $\vec{B}_{\rm xc}$ was still constrained to be parallel to $\vec{m}$ everywhere.[13–15]

C. Kagome lattice

Let us turn our attention to the second type of lattice considered in the present work, the kagome lattice. We have decided to examine this example using our formalism for two main reasons. First, this lattice exhibits interesting noncollinear spin arrangements, identification of which can further validate the quality of our approach. Second, materials that display this type of idealized lattice have been realized experimentally.[3,8,10] To the best of our knowledge, the theoretical treatment of these systems has not been attempted with realistic electronic structure Hamiltonians, but rather with models such as the Heisenberg Hamiltonian.[44–47] Because of the complex chemical environment in real materials, we believe that a fully *ab initio* treatment, as provided by our formalism, is important in studying such systems.

We have started our investigation with a three-atom magnetic unit cell. In this arrangement, we expect to identify two nonequivalent spin structures. These are known as the $\vec{q} = 0$ spin states,[48] which differ by the chirality of the spin magnetization, not by a global rotation in spin space. In the positive (negative) chirality, the magnetic moments are rotated clockwise (counterclockwise) when each of the triangles is traversed clockwise.[8] These lattices correspond to the classical ground states of the two-dimensional (2D) Heisenberg antiferromagnet with inclusion of interactions beyond the nearest neighbor (nn), which lifts the high degeneracy in the nn models.[49,50] The structure of the lattice is presented in Fig. 3. This figure also depicts the converged magnetic moments for the HISS functional. Because the spin space is independent of the geometry of the systems in our calculations, we have rotated the partitioned magnetization for the negative chirality to facilitate comparison with the positive one.

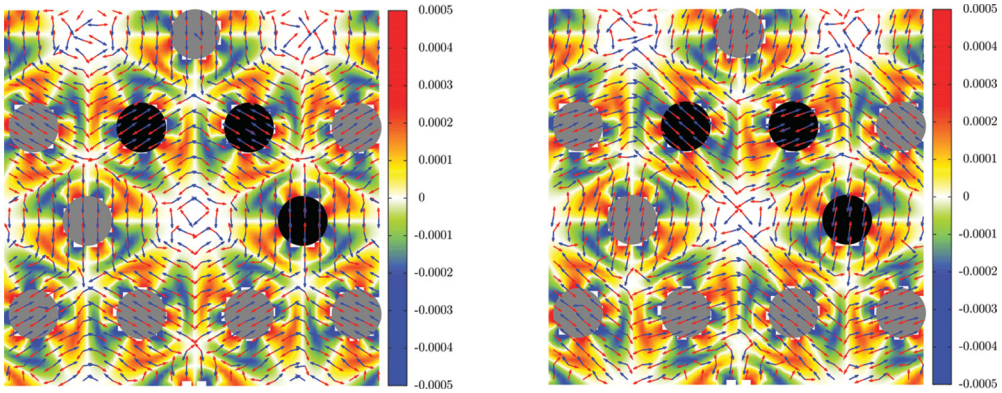

FIG. 4. (Color online) The directions of the magnetization (red arrows) and the exchange-correlation magnetic field (blue arrows) obtained with the PBE functional for the kagome lattice of (left) positive and (right) negative chirality. The color map depicts the magnitude (in atomic units) of $\vec{m} \times \vec{B}_{\rm xc}$ in the direction perpendicular to the Cr surface. The black points indicate the actual magnetic unit cell used in the calculations.

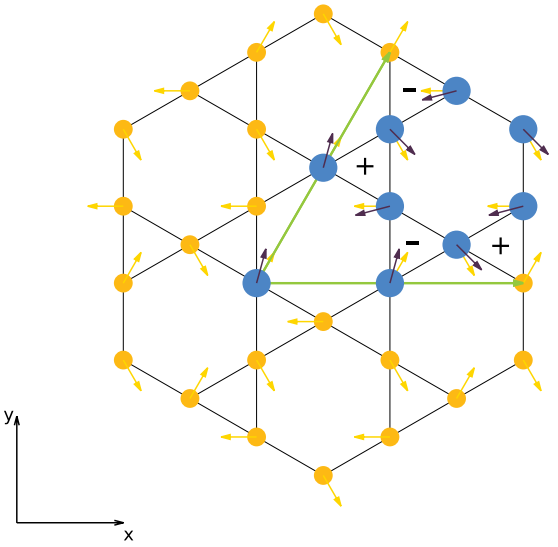

FIG. 5. (Color online) The structure of the $\sqrt{3} \times \sqrt{3}$ kagome lattice. The blue points represent the magnetic unit cell employed in the calculations, with arrows representing the converged magnetization obtained with the TPSS functional, partitioned according to the Hirshfeld scheme. Additionally, the translation vectors are presented (green arrows).

With all of the functionals employed, we have been able to identify these magnetic orderings. Additionally, we have found that all methods studied predict both chiral arrangements to be exactly degenerate, which is in agreement with the calculations based on the model Hamiltonians, without explicit inclusion of perturbations that can lift this degeneracy.[10,44] In agreement with the triangular lattice, the values of the atomic magnetic moments follow the rungs of Jacob's ladder. Again, the HISS functional is an exception, and its predictions of this quantity closely follow those of PBE. On the other hand, going from the triangular arrangement to the kagome lattice, we observe a significant increase of the norm of the magnetic moments. The values of the atomic magnetization obtained within the Hirshfeld approach are given in Table I.

In Fig. 4, we present the local distribution of the magnetization and exchange-correlation magnetic field. Once again, we notice a dominantly collinear arrangement in the core region with significant variations over the atomic boundaries. It is also clear that the high spin frustration of the underlying lattice gives rise to an interesting map of the local exchange-correlation magnetic torque, which could not have been captured with the previous generalization of collinear SDFT to the noncollinear regime.

Finally, let us discuss an alternative magnetic unit cell for the kagome lattice that we have employed in the present study. This is known as the $\sqrt{3} \times \sqrt{3}$ alignment, where corner-sharing triangles differ by chirality. The lattice, together with the magnetic unit cell, is presented in Fig. 5. This ordering is also a known ground state for the 2D Heisenberg Hamiltonian with beyond nearest-neighbor interactions. With all the methods studied, we succeeded in identifying solutions to the KS equations that correspond to this state. We have found that the atomic magnetic moments of the chromium atoms increase slightly compared to the $\vec{q} = 0$ states (please refer to Table I for actual values). This observation was confirmed by all XC functionals tested. The nonequivalent magnetic structure leads to a slightly different energy per site. We have found that the $\vec{q} = 0$ lattice is stabilized by 12, 14, 9, 3, and 15 meV per chromium atom with the LSDA, PBE, TPSS, HSE, and HISS functionals, respectively. Lifting the degeneracy between these two magnetic orderings has been also discussed in the literature[50] with the connection to the sign of the next-nearest-neighbor interaction.

IV. CONCLUSIONS

We have presented a generalization to periodic systems of the recently suggested extension of spin-density functional theory to the noncollinear regime. Our methodology is suitable for all commonly employed exchange-correlation density functionals, including successful range separated and screened ones. We have shown that our approach does not constrain the orientation between the magnetization and the exchange-correlation magnetic field. In other words, this extension does not suffer from the limitation of a vanishing local magnetic torque. We would like to stress the importance of this fact from the perspective of possible future spin-dynamics studies. Our approach is free of numerical instabilities. We have not encountered problems converging our equations to tight criteria.

We have applied our methodology to spin-frustrated atomistic lattice models. We believe that our approach, which allows applying accurate solid-state functionals in the noncollinear regime, will prove useful for calculations of magnetic properties. The formalism presented here can be readily employed in the study of other materials, including those containing f electrons. Results along these lines will be presented in due course.

ACKNOWLEDGMENTS

We would like to acknowledge Thomas M. Henderson for carefully reading the manuscript. The work at Rice University is supported by the DOE, Office of Basic Energy Sciences, Heavy Element Chemistry program, under Grant No. DE-FG02-04ER15523.

*ireneusz.bulik@rice.edu

[1] R. G. Parr and W. Yang, *Density-Functional Theory of Atoms and Molecules* (Oxford University Press, Oxford 1994).

[2] E. Engel and R. M. Dreizler, *Density-Functional Theory: An Advanced Course* (Springer, Heidelberg, 2011).

[3] D. Grohol, K. Matan, J.-H. Cho, S.-H. Lee, J. W. Lynn, D. G. Nocera, and Y. Lee, Nat. Mater. **4**, 323 (2005), and references therein.

[4] E.-Q. Gao, N. Liu, A.-L. Cheng, and S. Gao, Chem. Commun., 2470 (2007).

[5]K. W. Krämer, H. U. Güdel, B. Roessli, P. Fischer, A. Dönni, N. Wada, F. Fauth, M. T. Fernandez-Diaz, and T. Hauss, Phys. Rev. B **60**, R3724 (1999).
[6]J. J. Pulikkotil, L. Ke, M. van Schilfgaarde, T. Kotani, and V. P. Antropov, Supercond. Sci. Technol. **23**, 054012 (2010).
[7]P. Kurz, G. Bihlmayer, K. Hirai, and S. Blügel, Phys. Rev. Lett. **86**, 1106 (2001).
[8]T. Yildirim and A. B. Harris, Phys. Rev. B **73**, 214446 (2006).
[9]A. P. Ramirez, Annu. Rev. Mater. Sci. **24**, 453 (1994).
[10]K. Matan, B. M. Bartlett, J. S. Helton, V. Sikolenko, S. Mat'aš, K. Prokeš, Y. Chen, J. W. Lynn, D. Grohol, T. J. Sato, M. Tokunaga, D. G. Nocera, and Y. S. Lee, Phys. Rev. B **83**, 214406 (2011).
[11]U. von Barth and L. Hedin, J. Phys. C **5**, 1629 (1972).
[12]J. Kübler, K. H. Hock, J. Sticht, and A. R. Williams, J. Phys. F **18**, 469 (1988).
[13]P. Kurz, F. Förster, L. Nordström, G. Bihlmayer, and S. Blügel, Phys. Rev. B **69**, 024415 (2004).
[14]J. E. Peralta, G. E. Scuseria, and M. J. Frisch, Phys. Rev. B **75**, 125119 (2007).
[15]M. K. Armbruster, F. Weigend, C. van Wullen, and W. Klopper, PhysChemChemPhys **10**, 1748 (2008).
[16]G. Scalmani and M. J. Frisch, J. Chem. Theory Comput. **8**, 2193 (2012).
[17]K. Capelle, G. Vignale, and B. L. Györffy, Phys. Rev. Lett. **87**, 206403 (2001).
[18]S. Sharma, J. K. Dewhurst, C. Ambrosch-Draxl, S. Kurth, N. Helbig, S. Pittalis, S. Shallcross, L. Nordström, and E. K. U. Gross, Phys. Rev. Lett. **98**, 196405 (2007).
[19]J. Heyd, G. E. Scuseria, and M. Ernzerhof, J. Chem. Phys. **118**, 8207 (2003).
[20]J. Heyd, G. E. Scuseria, and M. Ernzerhof, J. Chem. Phys. **124**, 219906 (2006).
[21]J. Heyd and G. E. Scuseria, J. Chem. Phys. **120**, 7274 (2004).
[22]J. Heyd and G. E. Scuseria, J. Chem. Phys. **121**, 1187 (2004).
[23]T. M. Henderson, J. Paier, and G. E. Scuseria, Phys. Status Solidi B **248**, 767 (2011).
[24]M. J. Lucero, T. M. Henderson, and G. E. Scuseria, J. Phys. Condens. Matter **24**, 145504 (2012).
[25]J. A. Pople, P. M. Gill, and B. G. Johnson, Chem. Phys. Lett. **199**, 557 (1992).
[26]R. Seeger and J. A. Pople, J. Chem. Phys. **66**, 3045 (1977).
[27]C. A. Jimenez-Hoyos, T. M. Henderson, and G. E. Scuseria, J. Chem. Theory Comput. **7**, 2667 (2011).
[28]A. Seidl, A. Görling, P. Vogl, J. A. Majewski, and M. Levy, Phys. Rev. B **53**, 3764 (1996).
[29]V. N. Staroverov, G. E. Scuseria, and E. R. Davidson, J. Chem. Phys. **124**, 141103 (2006).
[30]K. N. Kudin and G. E. Scuseria, Chem. Phys. Lett. **283**, 61 (1998).
[31]K. N. Kudin and G. E. Scuseria, Chem. Phys. Lett. **289**, 611 (1998).
[32]M. C. Strain, G. E. Scuseria, and M. J. Frisch, Science **271**, 51 (1996).
[33]T. M. Henderson, A. F. Izmaylov, G. E. Scuseria, and A. Savin, J. Chem. Theory Comput. **4**, 1254 (2008).
[34]F. L. Hirshfeld, Theor. Chem. Acc. **44**, 129 (1977).
[35]M. Causà, in *Quantum-Mechanical Ab-initio Calculation of the Properties of Crystalline Materials* (Springer, Berlin, 1996), pp. 91–100.
[36]R. Stratmann, G. E. Scuseria, and M. J. Frisch, Chem. Phys. Lett. **257**, 213 (1996).
[37]E. Owen and E. Yates, Philos. Mag. Ser. 7 **16**, 606 (1933).
[38]S. H. Vosko, L. Wilk, and M. Nusair, Can. J. Phys. **58**, 1200 (1980).
[39]J. P. Perdew, K. Burke, and M. Ernzerhof, Phys. Rev. Lett. **77**, 3865 (1996).
[40]J. Tao, J. P. Perdew, V. N. Staroverov, and G. E. Scuseria, Phys. Rev. Lett. **91**, 146401 (2003).
[41]M. Dolg, U. Wedig, H. Stoll, and H. Preuss, J. Chem. Phys. **86**, 866 (1987).
[42]M. J. Frisch *et al.*, GAUSSIAN Development Version, revision H.22, Gaussian, Inc., Wallingford, CT, 2012.
[43]J. P. Perdew and K. Schmidt, AIP Conf. Proc. **577**, 1 (2001).
[44]M. Rigol and R. R. P. Singh, Phys. Rev. B **76**, 184403 (2007).
[45]O. Götze, D. J. J. Farnell, R. F. Bishop, P. H. Y. Li, and J. Richter, Phys. Rev. B **84**, 224428 (2011).
[46]L. Messio, B. Bernu, and C. Lhuillier, Phys. Rev. Lett. **108**, 207204 (2012).
[47]A. Mielke, J. Phys. A **25**, 4335 (1992).
[48]M. Nishiyama, S. Maegawa, T. Inami, and Y. Oka, Phys. Rev. B **67**, 224435 (2003).
[49]A. B. Harris, C. Kallin, and A. J. Berlinsky, Phys. Rev. B **45**, 2899 (1992).
[50]A. Chubukov, Phys. Rev. Lett. **69**, 832 (1992).